

Supporting Information

Cobalt oxide decked with inorganic-sulfur containing vanadium oxide for chromium (VI) reduction and UV-light assisted methyl orange degradation

Sayanika Saikia^a, Manoshi Saikia^a, Salma A. Khanam^a, Seonghwan Lee^b, Young-Bin Park^b, Lakshi Saikia^c, Gautam Gogoi^a, and Kusum K. Bania^{a*}

^aDepartment of Chemical Sciences, Tezpur University, Assam, India, 784028.

^bDepartment of Mechanical Engineering, Ulsan National Institute of Science and Technology, UNIST-gil 50, Ulju-gun, Ulsan 44919, Republic of Korea.

^cMaterials Science and Technology Division (MSTD), CSIR-North East Institute of Science and Technology, Jorhat 785006, Assam, India.

Corresponding Author

*Email: kusum@tezu.ernet.in or bania.kusum8@gmail.com.

ORCID

Kusum K. Bania: 0000-0001-6535-3913

Sl No.	Title	Page No.
1	Physical Measurements	S3-S4
2	DRS and Tauc's plot of S-VO _x and CoO _x , Fig. S1	S5
3	XPS of C(1s) of CoO _x -S-VO _x , Fig. S2	S6
4	EPR analysis and TGA analysis of CoO _x -S-VO _x , Fig. S3	S7
5	STEM-HAADF-EDX mapping of CoO _x -S-VO _x , Fig. S4	S8
6	Kinetics of Cr(VI) reduction, Fig. S5	S9
7	UV spectra and bar diagram of Cr(VI) reduction for different Cr solution concentration, Fig. S6	S10
8	Efficiency of S-VO _x , CoO _x , Co ₃ O ₄ -V ₂ O ₅ and CoO _x -S-VO _x material towards Cr(VI) reduction under optimized conditions, Fig. S7	S11
9	Cyclic voltamogram of Cr(VI) reduction with CoO _x -S-VO _x , Fig. S8	S12
10	Efficiency of CoO _x -S-VO _x towards MO degradation under normal laboratory condition and under dark, Fig. S9	S13
11	Efficiency of S-VO _x , CoO _x , Co ₃ O ₄ -V ₂ O ₅ and CoO _x -S-VO _x material towards MO degradation, Fig. S10	S14
12	UV spectra and bar diagram of MO degradation for different MO solution concentration, Fig. S11	S15
13	Point of zero charge (PZC) and effect of pH on MO degradation, Fig. S12	S16
14	Photoluminescence (PL) spectra, Fig. S13	S17
15	Ultraviolet photoelectron spectroscopy (UPS) analysis, Fig. S14	S18
16	Photocatalytic degradation mechanism using electron scavenger, hole scavenger and radical scavenger, Fig. S15	S19
17	Recyclability of CoO _x -S-VO _x , Fig. S16, S17, S18	S20-S21

1. Physical measurement

Physical measurements for different characterizations and analyses were done by the following techniques. The powder-X-ray diffraction (XRD) patterns were recorded in an instrument from BRUKER AXS, D8 FOCUS in the 2θ value range of $5-75^\circ$. The X-ray photoelectron (XPS) spectra were obtained from a XPS KRATOS (ESCA AXIS 165) spectrometer having Mg $K\alpha$ (1253.6 eV) as radiation source. Before transferring to the analysis chamber, the oven-dried sample was crushed into small pieces, sprinkled on a graphite sheet (double rod), and attached to a normal sample holder. The material was degassed overnight in a vacuum oven. The binding energy value was modified with reference to the 284.8 eV C 1s peak and the peak was deconvoluted using Origin software. Scanning Electron Microscope (SEM) images along with the X-Ray and Elemental mapping analyses were done SIGMA instrument manufactured by Carl Zeiss Microscopy. The Transmission Electron Microscope (TEM) images along with energy dispersive X-ray spectroscopy (EDX) analysis was performed on a JEM2010 (JEOL) instrument equipped with a slow scan CCD camera at an acceleration voltage of 200 kV. The UV-Vis experiments were carried out in Shimadzu, UV-2550 spectrophotometer. 500 mL of quartz glass chamber with a Mercury lamp, light source was surrounded by a double jacketed quartz immersion with an inlet and outlet of water circulation to ensure a safe temperature for the photocatalytic reaction. The infrared spectra had been recorded on a Perkin- Elmer 2000 FTIR spectrometer within the range of $450-4000\text{ cm}^{-1}$. The spectra of the solid samples were recorded as KBr pellets through blending the samples with KBr. The Diffuse Reflectance Spectra (DRS) were recorded employing a Hitachi U-3400 spectrophotometer. The cyclic voltammetry (CV) and Mott Schottky (MS) analysis studies were performed in a CHI-600E meter from CH

Instruments using the glassy carbon electrode (GCE) and Pt as a working electrode, Ag/AgCl as reference electrode and Pt wire as a counter electrode, respectively.

2. DRS and Tauc's plot of S-VO_x and CoO_x

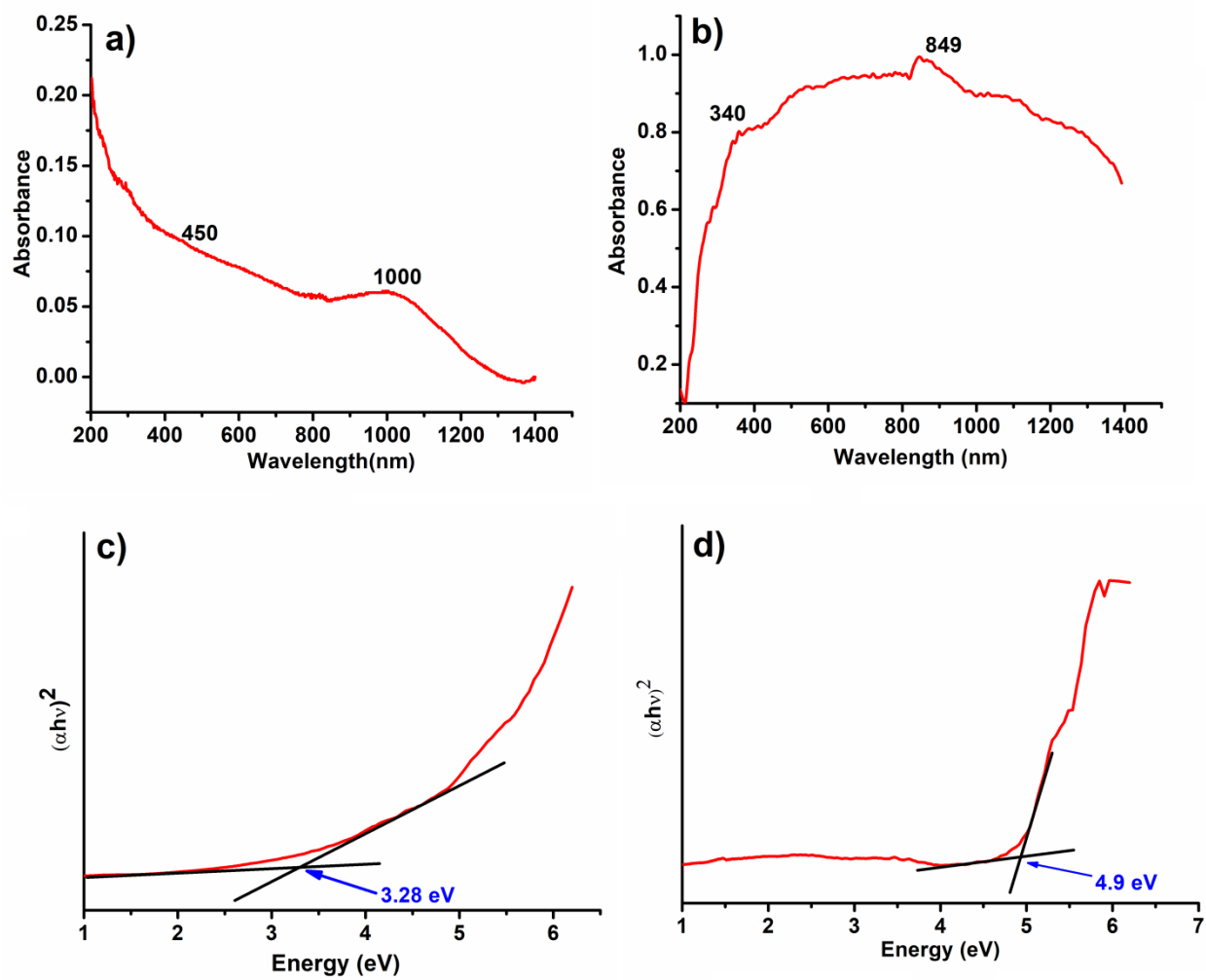


Fig. S1 DRS plot of a) CoO_x and b) S-VO_x, Tauc's plot of (a) CoO_x and (b) S-VO_x.

3. XPS of C(1s) of CoO_x-S-VO_x

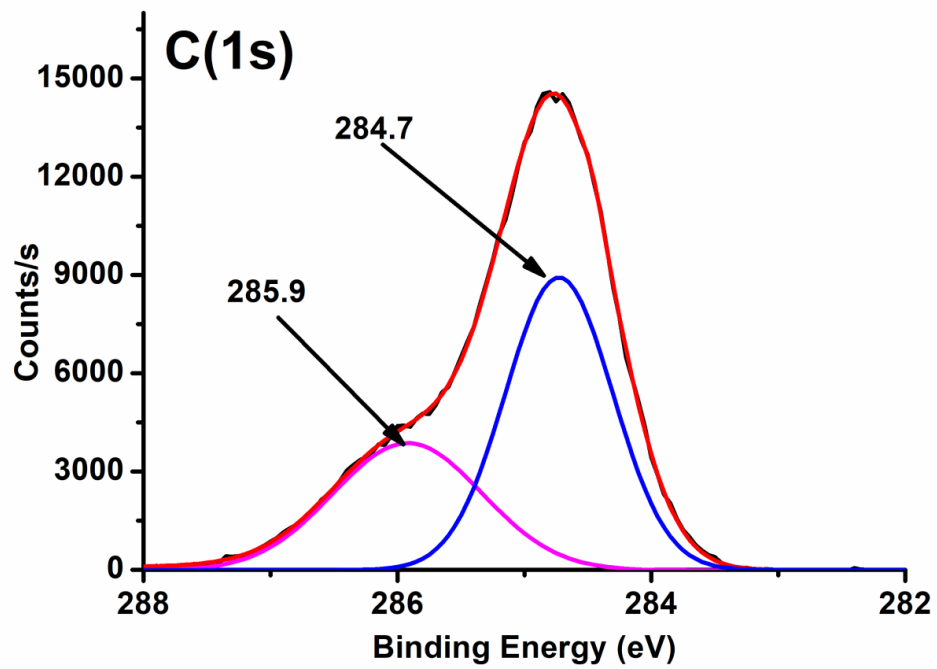


Fig. S2 XPS of C(1s) taken for peak fitting.

4. Electron Paramagnetic Resonance(EPR) spectra and Thermogravimetric Analysis(TGA) of $\text{CoO}_x\text{-S-VO}_x$ material.

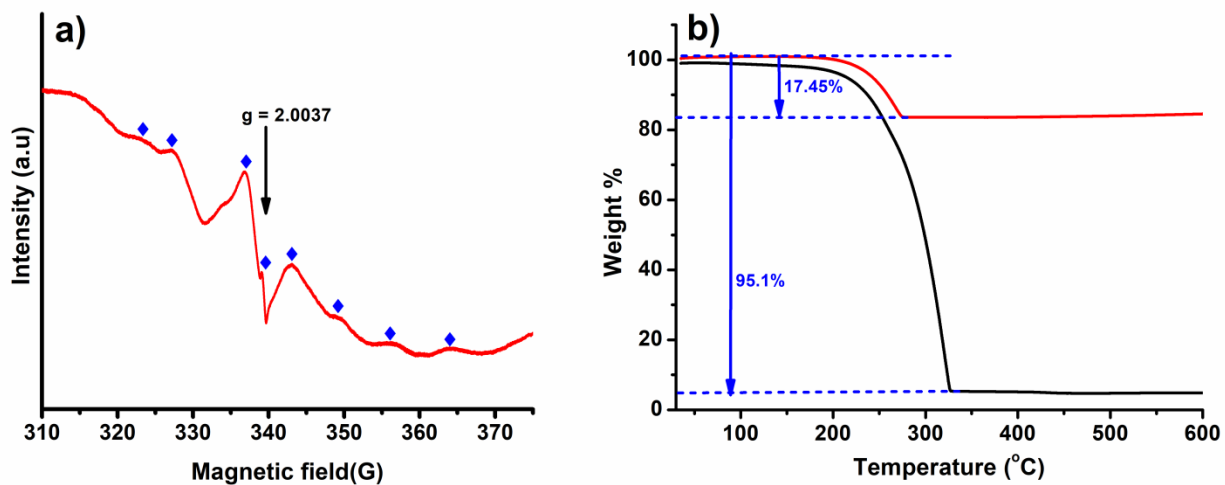


Fig. S3 (a)EPR spectra $\text{CoO}_x\text{-S-VO}_x$ and (b)TGA curve of $\text{CoO}_x\text{-S-VO}_x$ (red) and S-VO_x (black) material.

5. STEM-HAADF-EDX mapping of $\text{CoO}_x\text{-S-VO}_x$ material in different region.

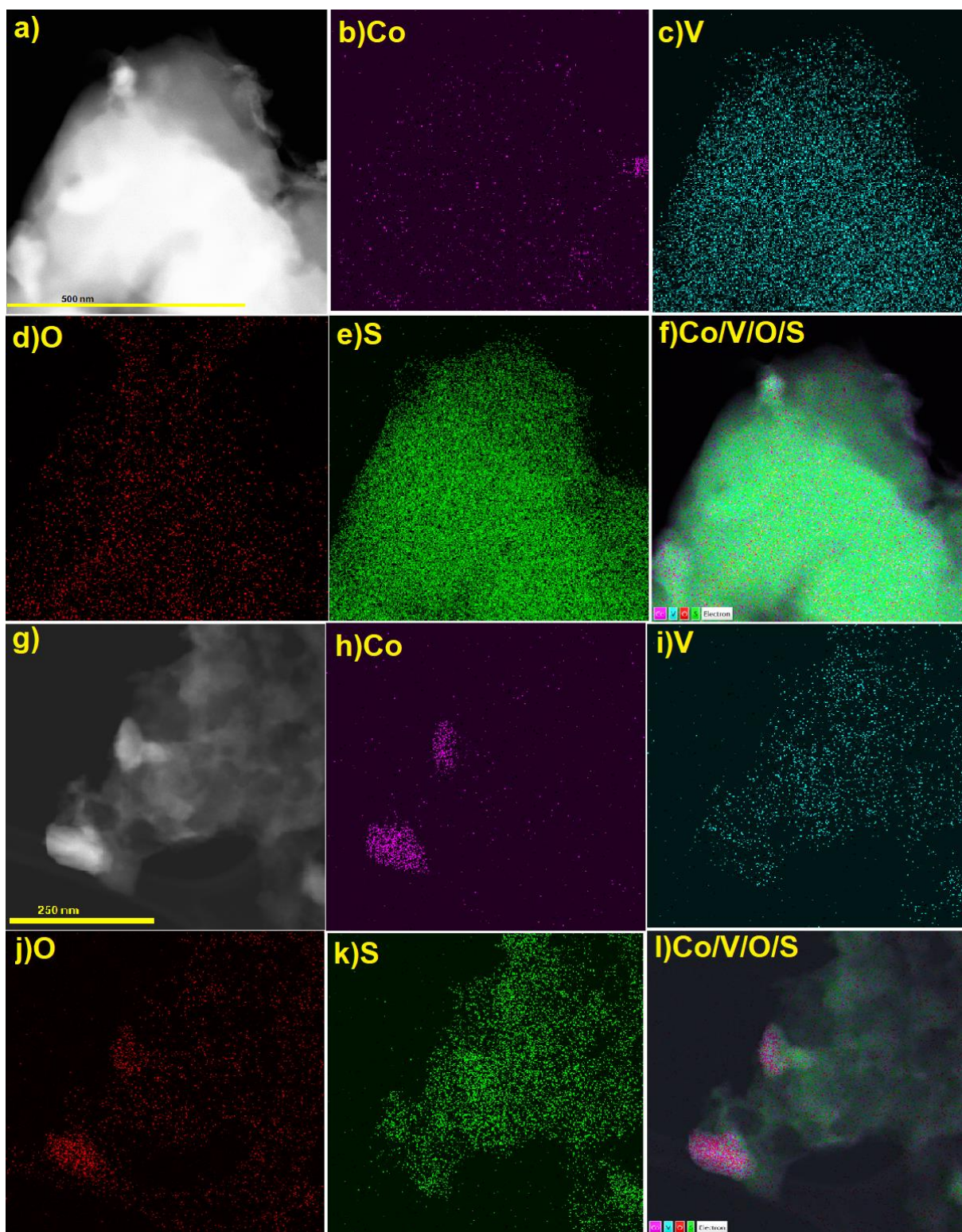


Fig. S4 STEM-HAADF-EDX mapping of $\text{CoO}_x\text{-S-VO}_x$ material in different region.

6. Kinetics of Cr(VI) reduction

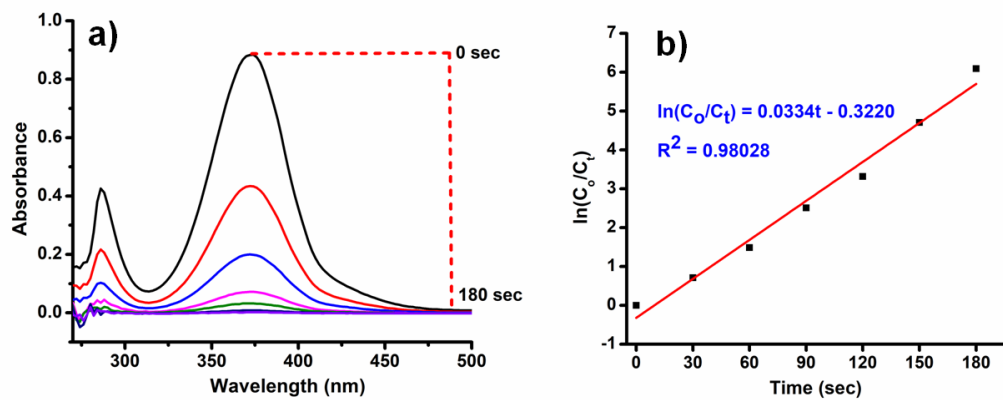


Fig. S5 (a) UV spectra recorded at 30 sec interval of time in optimized reaction condition and (b) $\ln(C_0/C_t)$ vs time graph showing kinetic study for Cr(VI) reduction.

7. UV spectra and bar diagram of Cr(VI) reduction for different Cr solution concentration with 10 mg CoO_x-S-VO_x and 1 mmol NaBH₄

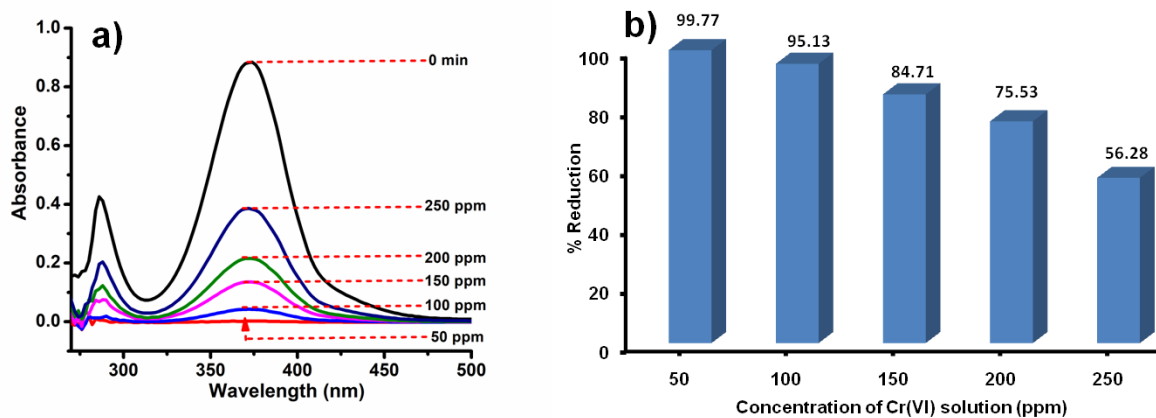


Fig. S6 (a) UV spectra and (b) bar diagram of Cr(VI) reduction for different Cr solution concentration.

8. Efficiency of S-VO_x, CoO_x, Co₃O₄-V₂O₅ and CoO_x-S-VO_x material towards Cr(VI) reduction under optimized conditions.

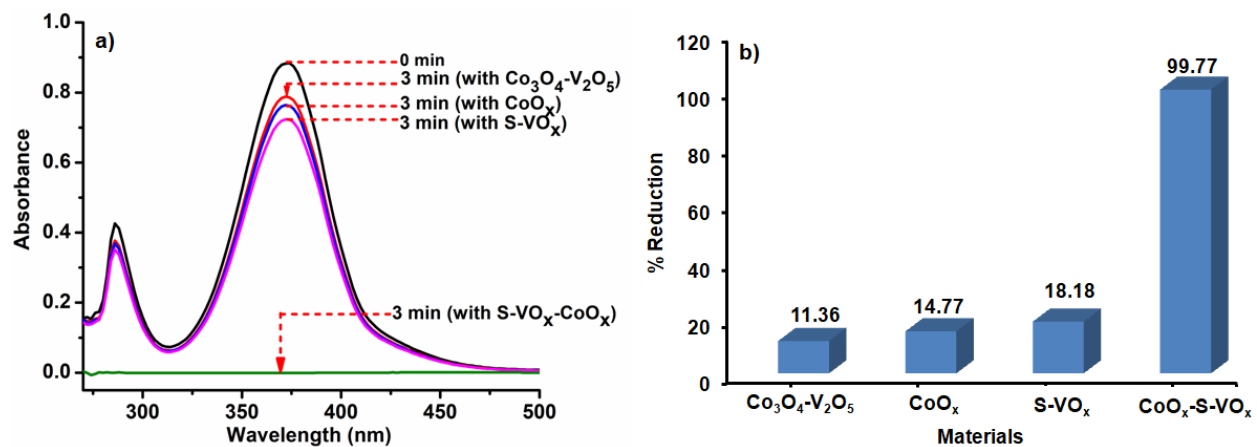


Fig. S7 (a) UV spectra and (b) bar diagram representing the Cr(VI) reduction efficiency with Co₃O₄-V₂O₅, CoO_x, S-VO_x and CoO_x-S-VO_x.

9. Cyclic voltamogram of Cr(VI) reduction with $\text{CoO}_x\text{-S-VO}_x$

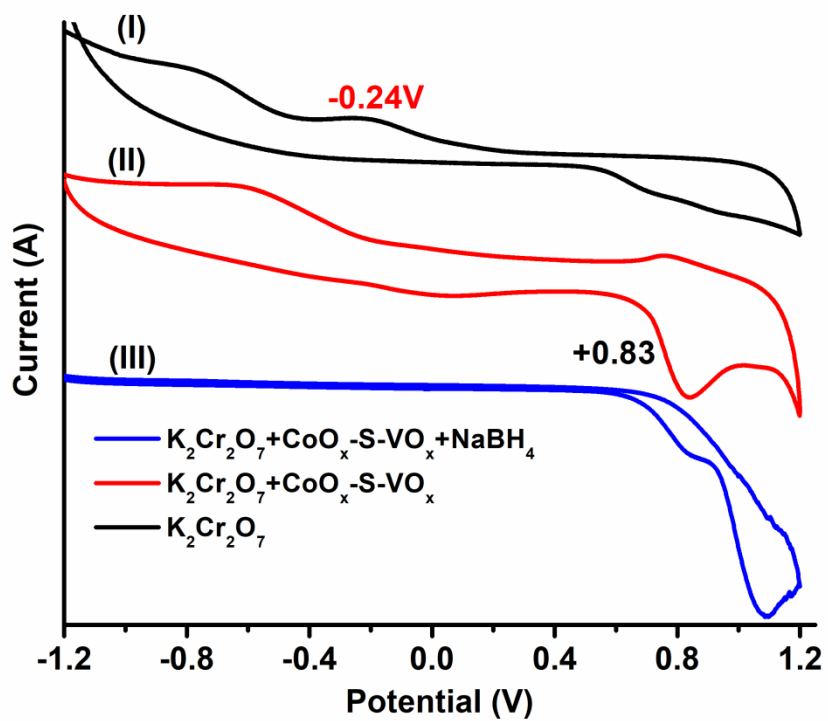


Fig. S8 CV of (I) $\text{K}_2\text{Cr}_2\text{O}_7$ (II) $\text{K}_2\text{Cr}_2\text{O}_7 + \text{CoO}_x\text{-S-VO}_x$ and (III) $\text{K}_2\text{Cr}_2\text{O}_7 + \text{CoO}_x\text{-S-VO}_x + \text{NaBH}_4$

10. Efficiency of CoO_x-S-VO_x towards MO degradation under normal laboratory condition and under dark.

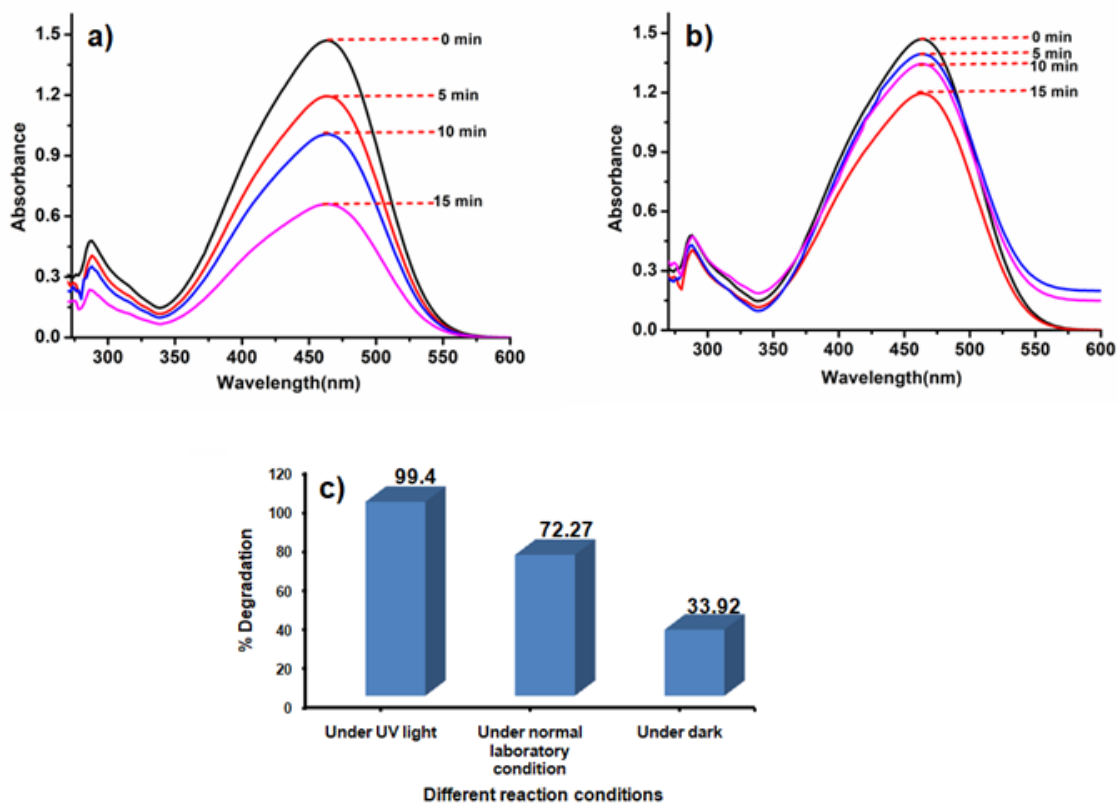


Fig. S9 MO degradation efficiency with CoO_x-S-VO_x (a) under normal laboratory condition, (b) under dark, (c) comparative bar diagram for MO degradation efficiency with CoO_x-S-VO_x upto 40 min.

11. Efficiency of S-VO_x, CoO_x, Co₃O₄-V₂O₅ and CoO_x-S-VO_x material towards MO degradation

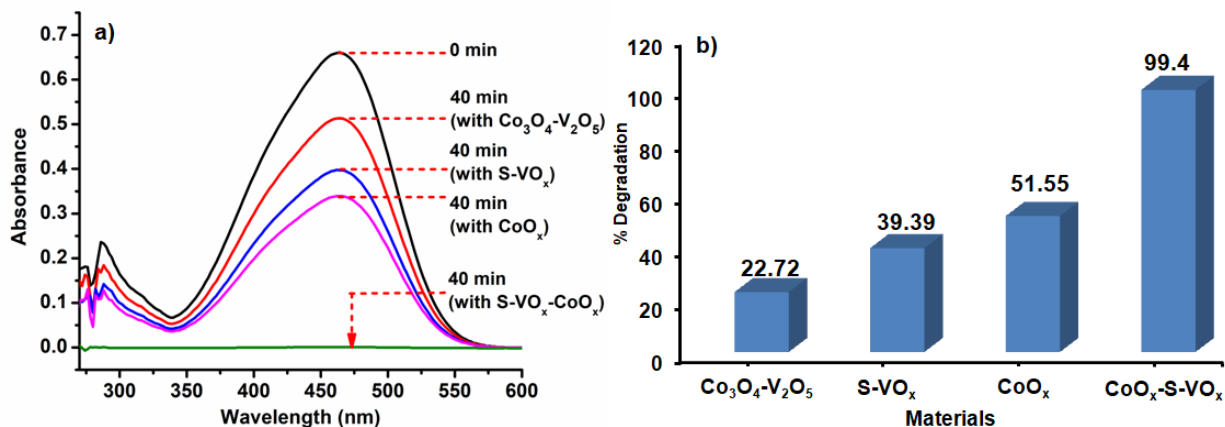


Fig. S10 (a) UV spectra and (b) bar diagram representing the MO degradation efficiency with Co₃O₄-V₂O₅, S-VO_x, CoO_x and CoO_x-S-VO_x.

12. UV spectra and bar diagram of MO degradation for different MO solution concentration

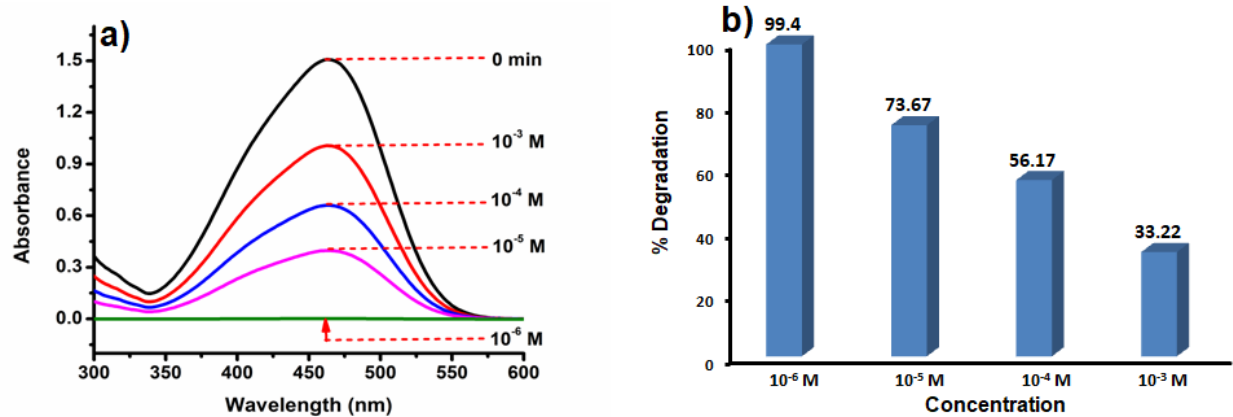


Fig. S11 (a) UV spectra and (b) bar diagram of MO degradation for different MO solution concentration.

13. Point of Zero Charge (PZC) determination and effect of pH on MO degradation with $\text{CoO}_x\text{-S-VO}_x$.

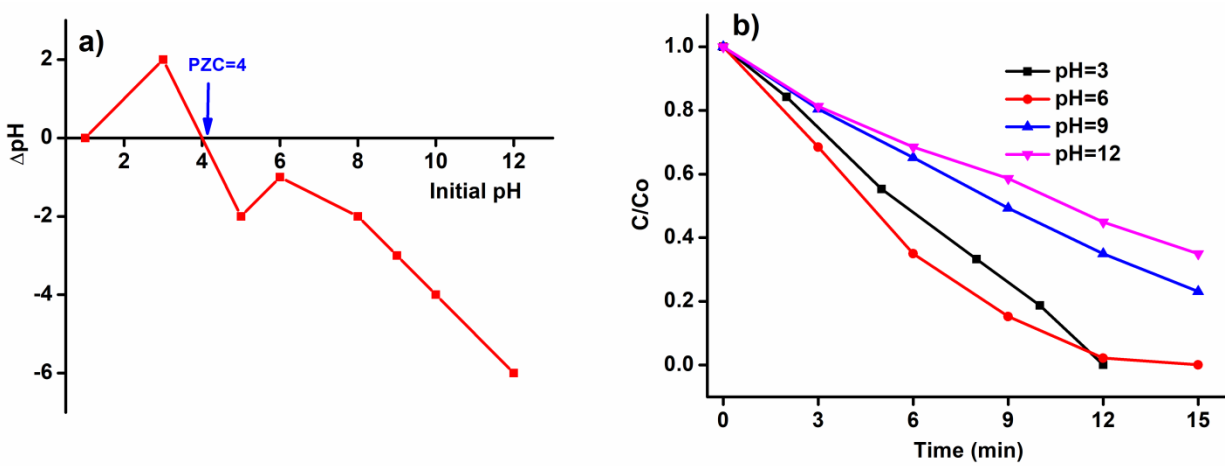


Fig. S12 (a) Point of zero charge of $\text{CoO}_x\text{-S-VO}_x$ material and (b) efficiency of MO degradation at different pH.

14. Photoluminescence (PL) Spectra

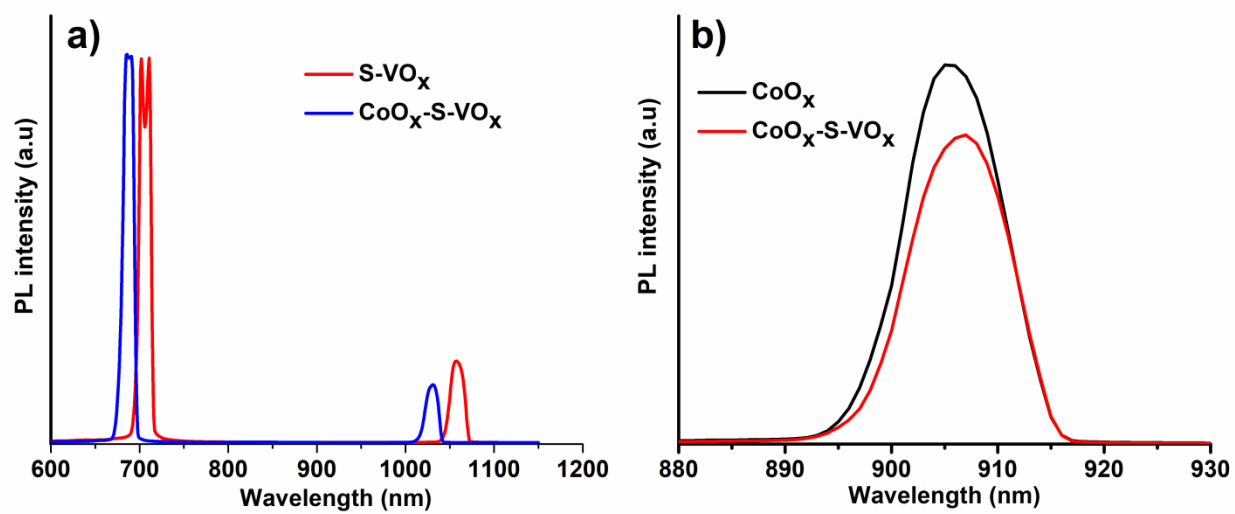


Fig. S13 PL spectra recorded at excitation wavelength of (a) 450 nm and (b) 740 nm

15. Ultraviolet Photoelectron Spectroscopy (UPS) analysis.

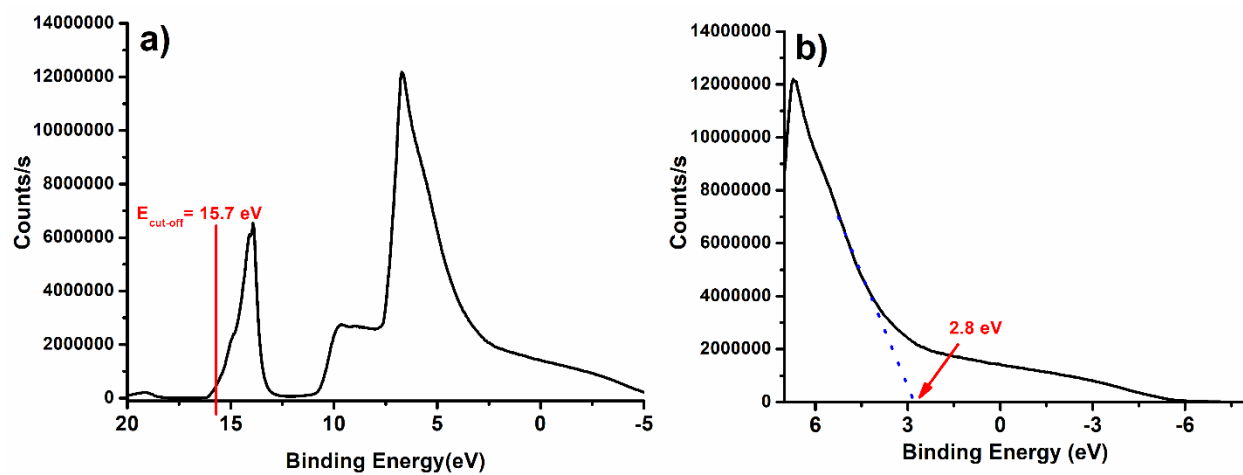


Fig. S14 a) UPS spectra and b) Valence band energy of $\text{CoO}_x\text{-S-VO}_x$

16. Photocatalytic degradation mechanism using electron scavenger (AgNO_3), hole scavenger (KI) and OH^\bullet radical scavenger (isopropanol) and O_2^\bullet radical scavenger (ascorbic acid)

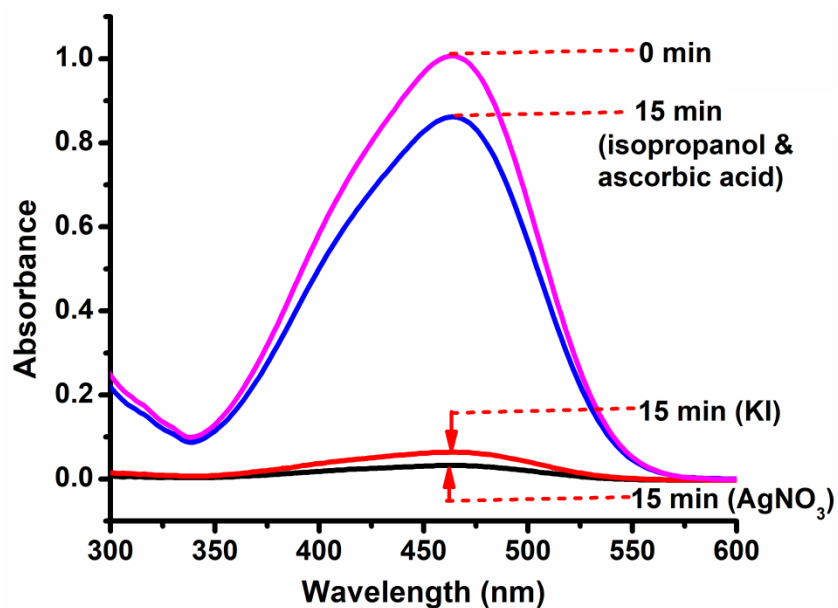


Fig. S15 Photocatalytic degradation mechanism using electron scavenger (AgNO_3), hole scavenger (KI) and OH^\bullet radical scavenger (isopropanol) and O_2^\bullet radical scavenger (ascorbic acid).

17. Recyclability test of $\text{CoO}_x\text{-S-VO}_x$

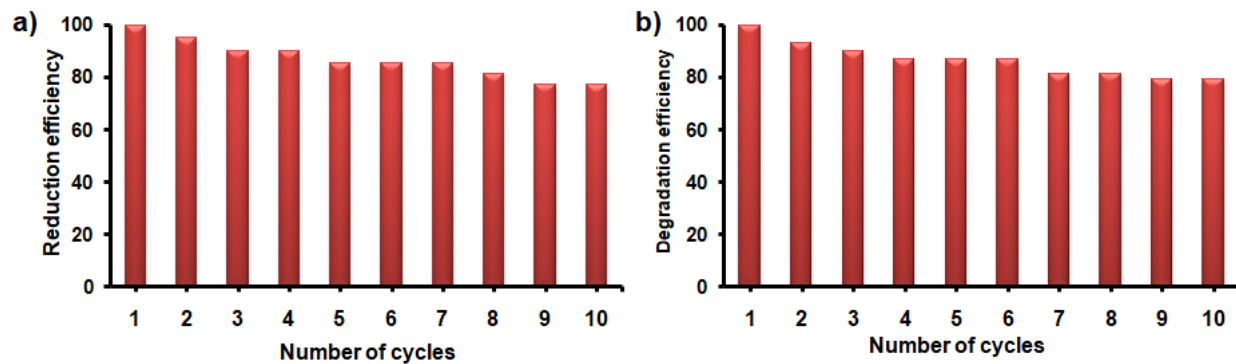


Fig. S16 Recyclable efficiency of $\text{CoO}_x\text{-S-VO}_x$ in case of (a) Cr(VI) reduction and (b) MO degradation.

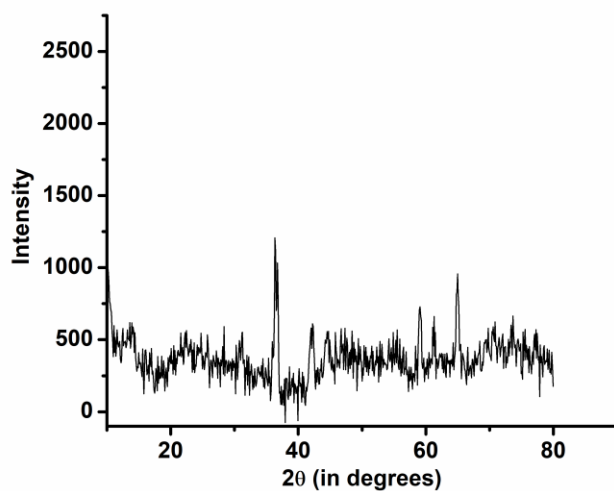


Fig. S17 PXRD spectra of recycled $\text{CoO}_x\text{-S-VO}_x$ catalyst after 10th cycle.

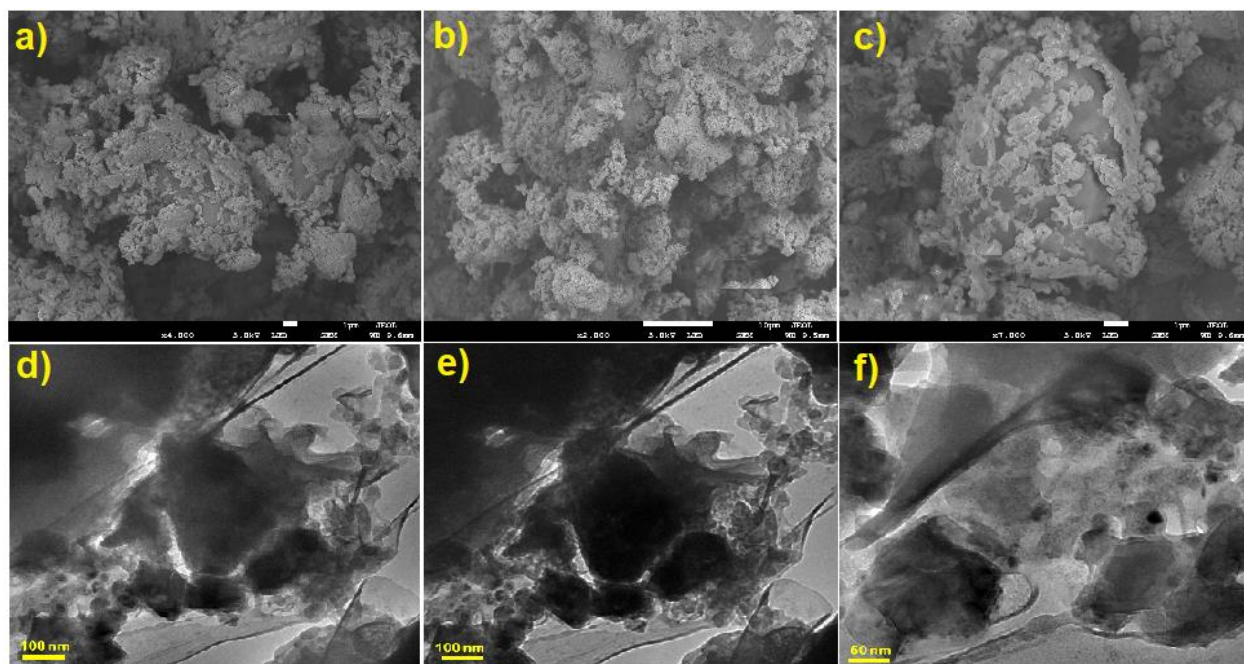


Fig. S18 (a-c) SEM images and (d-f) TEM images of recycled $\text{CoO}_x\text{-S-VO}_x$ catalyst after 10th cycle.